

# Beam energy dependence of moments of the net-charge multiplicity distributions in Au+Au collisions at RHIC

L. Adamczyk,<sup>1</sup> J. K. Adkins,<sup>23</sup> G. Agakishiev,<sup>21</sup> M. M. Aggarwal,<sup>35</sup> Z. Ahammed,<sup>54</sup> I. Alekseev,<sup>19</sup> J. Alford,<sup>22</sup> C. D. Anson,<sup>32</sup> A. Aparin,<sup>21</sup> D. Arkhipkin,<sup>4</sup> E. C. Aschenauer,<sup>4</sup> G. S. Averichev,<sup>21</sup> J. Balewski,<sup>27</sup> A. Banerjee,<sup>54</sup> Z. Barnovska,<sup>14</sup> D. R. Beavis,<sup>4</sup> R. Bellwied,<sup>50</sup> A. Bhasin,<sup>20</sup> A. K. Bhati,<sup>35</sup> P. Bhattarai,<sup>49</sup> H. Bichsel,<sup>56</sup> J. Bielcik,<sup>13</sup> J. Bielcikova,<sup>14</sup> L. C. Bland,<sup>4</sup> I. G. Bordyuzhin,<sup>19</sup> W. Borowski,<sup>46</sup> J. Bouchet,<sup>22</sup> A. V. Brandin,<sup>30</sup> S. G. Brovko,<sup>6</sup> S. Bültmann,<sup>33</sup> I. Bunzarov,<sup>21</sup> T. P. Burton,<sup>4</sup> J. Butterworth,<sup>41</sup> H. Caines,<sup>57</sup> M. Calderón de la Barca Sánchez,<sup>6</sup> D. Cebra,<sup>6</sup> R. Cendejas,<sup>36</sup> M. C. Cervantes,<sup>48</sup> P. Chaloupka,<sup>13</sup> Z. Chang,<sup>48</sup> S. Chatopadhyay,<sup>54</sup> H. F. Chen,<sup>43</sup> J. H. Chen,<sup>45</sup> L. Chen,<sup>9</sup> J. Cheng,<sup>51</sup> M. Cherney,<sup>12</sup> A. Chikanian,<sup>57</sup> W. Christie,<sup>4</sup> J. Chwastowski,<sup>11</sup> M. J. M. Codrington,<sup>49</sup> R. Corliss,<sup>27</sup> J. G. Cramer,<sup>56</sup> H. J. Crawford,<sup>5</sup> X. Cui,<sup>43</sup> S. Das,<sup>16</sup> A. Davila Leyva,<sup>49</sup> L. C. De Silva,<sup>50</sup> R. R. Debbe,<sup>4</sup> T. G. Dedovich,<sup>21</sup> J. Deng,<sup>44</sup> A. A. Derevschikov,<sup>37</sup> R. Derradi de Souza,<sup>8</sup> S. Dhamija,<sup>18</sup> B. di Ruzza,<sup>4</sup> L. Didenko,<sup>4</sup> C. Dilks,<sup>36</sup> F. Ding,<sup>6</sup> P. Djawotho,<sup>48</sup> X. Dong,<sup>26</sup> J. L. Drachenberg,<sup>53</sup> J. E. Draper,<sup>6</sup> C. M. Du,<sup>25</sup> L. E. Dunkelberger,<sup>7</sup> J. C. Dunlop,<sup>4</sup> L. G. Efimov,<sup>21</sup> J. Engelage,<sup>5</sup> K. S. Engle,<sup>52</sup> G. Eppley,<sup>41</sup> L. Eun,<sup>26</sup> O. Evdokimov,<sup>10</sup> R. Fatemi,<sup>23</sup> S. Fazio,<sup>4</sup> J. Fedorisin,<sup>21</sup> P. Filip,<sup>21</sup> E. Finch,<sup>57</sup> Y. Fisyak,<sup>4</sup> C. E. Flores,<sup>6</sup> C. A. Gagliardi,<sup>48</sup> D. R. Gangadharan,<sup>32</sup> D. Garand,<sup>38</sup> F. Geurts,<sup>41</sup> A. Gibson,<sup>53</sup> M. Girard,<sup>55</sup> S. Gliske,<sup>2</sup> D. Grosnick,<sup>53</sup> Y. Guo,<sup>43</sup> A. Gupta,<sup>20</sup> S. Gupta,<sup>20</sup> W. Guryn,<sup>4</sup> B. Haag,<sup>6</sup> O. Hajkova,<sup>13</sup> A. Hamed,<sup>48</sup> L-X. Han,<sup>45</sup> R. Haque,<sup>31</sup> J. W. Harris,<sup>57</sup> J. P. Hays-Wehle,<sup>27</sup> S. Heppelmann,<sup>36</sup> A. Hirsch,<sup>38</sup> G. W. Hoffmann,<sup>49</sup> D. J. Hofman,<sup>10</sup> S. Horvat,<sup>57</sup> B. Huang,<sup>4</sup> H. Z. Huang,<sup>7</sup> P. Huck,<sup>9</sup> T. J. Humanic,<sup>32</sup> G. Igo,<sup>7</sup> W. W. Jacobs,<sup>18</sup> H. Jang,<sup>24</sup> E. G. Judd,<sup>5</sup> S. Kabana,<sup>46</sup> D. Kalinkin,<sup>19</sup> K. Kang,<sup>51</sup> K. Kauder,<sup>10</sup> H. W. Ke,<sup>9</sup> D. Keane,<sup>22</sup> A. Kechechyan,<sup>21</sup> A. Kesich,<sup>6</sup> Z. H. Khan,<sup>10</sup> D. P. Kikola,<sup>38</sup> I. Kisiel,<sup>15</sup> A. Kisiel,<sup>55</sup> D. D. Koetke,<sup>53</sup> T. Kollegger,<sup>15</sup> J. Konzer,<sup>38</sup> I. Koralt,<sup>33</sup> W. Korsch,<sup>23</sup> L. Kotchenda,<sup>30</sup> P. Kravtsov,<sup>30</sup> K. Krueger,<sup>2</sup> I. Kulakov,<sup>15</sup> L. Kumar,<sup>31</sup> R. A. Kycia,<sup>11</sup> M. A. C. Lamont,<sup>4</sup> J. M. Landgraf,<sup>4</sup> K. D. Landry,<sup>7</sup> J. Lauret,<sup>4</sup> A. Lebedev,<sup>4</sup> R. Lednický,<sup>21</sup> J. H. Lee,<sup>4</sup> W. Leight,<sup>27</sup> M. J. LeVine,<sup>4</sup> C. Li,<sup>43</sup> W. Li,<sup>45</sup> X. Li,<sup>38</sup> X. Li,<sup>47</sup> Y. Li,<sup>51</sup> Z. M. Li,<sup>9</sup> L. M. Lima,<sup>42</sup> M. A. Lisa,<sup>32</sup> F. Liu,<sup>9</sup> T. Ljubicic,<sup>4</sup> W. J. Llope,<sup>41</sup> R. S. Longacre,<sup>4</sup> X. Luo,<sup>9</sup> G. L. Ma,<sup>45</sup> Y. G. Ma,<sup>45</sup> D. M. M. D. Madagodagettige Don,<sup>12</sup> D. P. Mahapatra,<sup>16</sup> R. Majka,<sup>57</sup> S. Margetis,<sup>22</sup> C. Markert,<sup>49</sup> H. Masui,<sup>26</sup> H. S. Matis,<sup>26</sup> D. McDonald,<sup>41</sup> T. S. McShane,<sup>12</sup> N. G. Minaev,<sup>37</sup> S. Mioduszewski,<sup>48</sup> B. Mohanty,<sup>31</sup> M. M. Mondal,<sup>48</sup> D. A. Morozov,<sup>37</sup> M. G. Munhoz,<sup>42</sup> M. K. Mustafa,<sup>38</sup> B. K. Nandi,<sup>17</sup> Md. Nasim,<sup>31</sup> T. K. Nayak,<sup>54</sup> J. M. Nelson,<sup>3</sup> L. V. Nogach,<sup>37</sup> S. Y. Noh,<sup>24</sup> J. Novak,<sup>29</sup> S. B. Nurushev,<sup>37</sup> G. Odyniec,<sup>26</sup> A. Ogawa,<sup>4</sup> K. Oh,<sup>39</sup> A. Ohlson,<sup>57</sup> V. Okorokov,<sup>30</sup> E. W. Oldag,<sup>49</sup> R. A. N. Oliveira,<sup>42</sup> M. Pachr,<sup>13</sup> B. S. Page,<sup>18</sup> S. K. Pal,<sup>54</sup> Y. X. Pan,<sup>7</sup> Y. Pandit,<sup>10</sup> Y. Panebratsev,<sup>21</sup> T. Pawlak,<sup>55</sup> B. Pawlik,<sup>34</sup> H. Pei,<sup>9</sup> C. Perkins,<sup>5</sup> W. Peryt,<sup>55</sup> A. Peterson,<sup>32</sup> P. Pile,<sup>4</sup> M. Planinic,<sup>58</sup> J. Pluta,<sup>55</sup> D. Plyku,<sup>33</sup> N. Poljak,<sup>58</sup> J. Porter,<sup>26</sup> A. M. Poskanzer,<sup>26</sup> N. K. Pruthi,<sup>35</sup> M. Przybycien,<sup>1</sup> P. R. Pujahari,<sup>17</sup> H. Qiu,<sup>26</sup> A. Quintero,<sup>22</sup> S. Ramachandran,<sup>23</sup> R. Raniwala,<sup>40</sup> S. Raniwala,<sup>40</sup> R. L. Ray,<sup>49</sup> C. K. Riley,<sup>57</sup> H. G. Ritter,<sup>26</sup> J. B. Roberts,<sup>41</sup> O. V. Rogachevskiy,<sup>21</sup> J. L. Romero,<sup>6</sup> J. F. Ross,<sup>12</sup> A. Roy,<sup>54</sup> L. Ruan,<sup>4</sup> J. Rusnak,<sup>14</sup> N. R. Sahoo,<sup>54</sup> P. K. Sahu,<sup>16</sup> I. Sakrejda,<sup>26</sup> S. Salur,<sup>26</sup> A. Sandacz,<sup>55</sup> J. Sandweiss,<sup>57</sup> E. Sangaline,<sup>6</sup> A. Sarkar,<sup>17</sup> J. Schambach,<sup>49</sup> R. P. Scharenberg,<sup>38</sup> A. M. Schmah,<sup>26</sup> W. B. Schmidke,<sup>4</sup> N. Schmitz,<sup>28</sup> J. Seger,<sup>12</sup> P. Seyboth,<sup>28</sup> N. Shah,<sup>7</sup> E. Shahaliev,<sup>21</sup> P. V. Shanmuganathan,<sup>22</sup> M. Shao,<sup>43</sup> B. Sharma,<sup>35</sup> W. Q. Shen,<sup>45</sup> S. S. Shi,<sup>26</sup> Q. Y. Shou,<sup>45</sup> E. P. Sichtermann,<sup>26</sup> R. N. Singaraju,<sup>54</sup> M. J. Skoby,<sup>18</sup> D. Smirnov,<sup>4</sup> N. Smirnov,<sup>57</sup> D. Solanki,<sup>40</sup> P. Sorensen,<sup>4</sup> U. G. deSouza,<sup>42</sup> H. M. Spinka,<sup>2</sup> B. Srivastava,<sup>38</sup> T. D. S. Stanislaus,<sup>53</sup> J. R. Stevens,<sup>27</sup> R. Stock,<sup>15</sup> M. Strikhanov,<sup>30</sup> B. Stringfellow,<sup>38</sup> A. A. P. Suaide,<sup>42</sup> M. Sumbera,<sup>14</sup> X. Sun,<sup>26</sup> X. M. Sun,<sup>26</sup> Y. Sun,<sup>43</sup> Z. Sun,<sup>25</sup> B. Surrow,<sup>47</sup> D. N. Svirida,<sup>19</sup> T. J. M. Symons,<sup>26</sup> A. Szanto de Toledo,<sup>42</sup> J. Takahashi,<sup>8</sup> A. H. Tang,<sup>4</sup> Z. Tang,<sup>43</sup> T. Tarnowsky,<sup>29</sup> J. H. Thomas,<sup>26</sup> A. R. Timmins,<sup>50</sup> D. Tlusty,<sup>14</sup> M. Tokarev,<sup>21</sup> S. Trentalange,<sup>7</sup> R. E. Tribble,<sup>48</sup> P. Tribedy,<sup>54</sup> B. A. Trzeciak,<sup>55</sup> O. D. Tsai,<sup>7</sup> J. Turnau,<sup>34</sup> T. Ullrich,<sup>4</sup> D. G. Underwood,<sup>2</sup> G. Van Buren,<sup>4</sup> G. van Nieuwenhuizen,<sup>27</sup> J. A. Vanfossen, Jr.,<sup>22</sup> R. Varma,<sup>17</sup> G. M. S. Vasconcelos,<sup>8</sup> A. N. Vasiliev,<sup>37</sup> R. Vertesi,<sup>14</sup> F. Videbæk,<sup>4</sup> Y. P. Viyogi,<sup>54</sup> S. Vokal,<sup>21</sup> A. Vossen,<sup>18</sup> M. Wada,<sup>49</sup> M. Walker,<sup>27</sup> F. Wang,<sup>38</sup> G. Wang,<sup>7</sup> H. Wang,<sup>4</sup> J. S. Wang,<sup>25</sup> X. L. Wang,<sup>43</sup> Y. Wang,<sup>51</sup> Y. Wang,<sup>10</sup> G. Webb,<sup>23</sup> J. C. Webb,<sup>4</sup> G. D. Westfall,<sup>29</sup> H. Wieman,<sup>26</sup> S. W. Wissink,<sup>18</sup> R. Witt,<sup>52</sup> Y. F. Wu,<sup>9</sup> Z. Xiao,<sup>51</sup> W. Xie,<sup>38</sup> K. Xin,<sup>41</sup> H. Xu,<sup>25</sup> N. Xu,<sup>26</sup> Q. H. Xu,<sup>44</sup> Y. Xu,<sup>43</sup> Z. Xu,<sup>4</sup> W. Yan,<sup>51</sup> C. Yang,<sup>43</sup> Y. Yang,<sup>25</sup> Y. Yang,<sup>9</sup> Z. Ye,<sup>10</sup> P. Yépez,<sup>41</sup> L. Yi,<sup>38</sup> K. Yip,<sup>4</sup> I-K. Yoo,<sup>39</sup> Y. Zawisza,<sup>43</sup> H. Zbroszczyk,<sup>55</sup> W. Zha,<sup>43</sup> J. B. Zhang,<sup>9</sup> S. Zhang,<sup>45</sup> X. P. Zhang,<sup>51</sup> Y. Zhang,<sup>43</sup> Z. P. Zhang,<sup>43</sup> F. Zhao,<sup>7</sup> J. Zhao,<sup>45</sup> C. Zhong,<sup>45</sup> X. Zhu,<sup>51</sup> Y. H. Zhu,<sup>45</sup> Y. Zoukarneeva,<sup>21</sup> and M. Zyzak<sup>15</sup>

(STAR Collaboration)

- <sup>1</sup>AGH University of Science and Technology, Cracow, Poland  
<sup>2</sup>Argonne National Laboratory, Argonne, Illinois 60439, USA  
<sup>3</sup>University of Birmingham, Birmingham, United Kingdom  
<sup>4</sup>Brookhaven National Laboratory, Upton, New York 11973, USA  
<sup>5</sup>University of California, Berkeley, California 94720, USA  
<sup>6</sup>University of California, Davis, California 95616, USA  
<sup>7</sup>University of California, Los Angeles, California 90095, USA  
<sup>8</sup>Universidade Estadual de Campinas, Sao Paulo, Brazil  
<sup>9</sup>Central China Normal University (HZNU), Wuhan 430079, China  
<sup>10</sup>University of Illinois at Chicago, Chicago, Illinois 60607, USA  
<sup>11</sup>Cracow University of Technology, Cracow, Poland  
<sup>12</sup>Creighton University, Omaha, Nebraska 68178, USA  
<sup>13</sup>Czech Technical University in Prague, FNSPE, Prague, 115 19, Czech Republic  
<sup>14</sup>Nuclear Physics Institute AS CR, 250 68 Řež/Prague, Czech Republic  
<sup>15</sup>Frankfurt Institute for Advanced Studies FIAS, Germany  
<sup>16</sup>Institute of Physics, Bhubaneswar 751005, India  
<sup>17</sup>Indian Institute of Technology, Mumbai, India  
<sup>18</sup>Indiana University, Bloomington, Indiana 47408, USA  
<sup>19</sup>Alikhanov Institute for Theoretical and Experimental Physics, Moscow, Russia  
<sup>20</sup>University of Jammu, Jammu 180001, India  
<sup>21</sup>Joint Institute for Nuclear Research, Dubna, 141 980, Russia  
<sup>22</sup>Kent State University, Kent, Ohio 44242, USA  
<sup>23</sup>University of Kentucky, Lexington, Kentucky, 40506-0055, USA  
<sup>24</sup>Korea Institute of Science and Technology Information, Daejeon, Korea  
<sup>25</sup>Institute of Modern Physics, Lanzhou, China  
<sup>26</sup>Lawrence Berkeley National Laboratory, Berkeley, California 94720, USA  
<sup>27</sup>Massachusetts Institute of Technology, Cambridge, MA 02139-4307, USA  
<sup>28</sup>Max-Planck-Institut für Physik, Munich, Germany  
<sup>29</sup>Michigan State University, East Lansing, Michigan 48824, USA  
<sup>30</sup>Moscow Engineering Physics Institute, Moscow Russia  
<sup>31</sup>National Institute of Science Education and Research, Bhubaneswar 751005, India  
<sup>32</sup>Ohio State University, Columbus, Ohio 43210, USA  
<sup>33</sup>Old Dominion University, Norfolk, VA, 23529, USA  
<sup>34</sup>Institute of Nuclear Physics PAN, Cracow, Poland  
<sup>35</sup>Panjab University, Chandigarh 160014, India  
<sup>36</sup>Pennsylvania State University, University Park, Pennsylvania 16802, USA  
<sup>37</sup>Institute of High Energy Physics, Protvino, Russia  
<sup>38</sup>Purdue University, West Lafayette, Indiana 47907, USA  
<sup>39</sup>Pusan National University, Pusan, Republic of Korea  
<sup>40</sup>University of Rajasthan, Jaipur 302004, India  
<sup>41</sup>Rice University, Houston, Texas 77251, USA  
<sup>42</sup>Universidade de São Paulo, São Paulo, Brazil  
<sup>43</sup>University of Science & Technology of China, Hefei 230026, China  
<sup>44</sup>Shandong University, Jinan, Shandong 250100, China  
<sup>45</sup>Shanghai Institute of Applied Physics, Shanghai 201800, China  
<sup>46</sup>SUBATECH, Nantes, France  
<sup>47</sup>Temple University, Philadelphia, Pennsylvania, 19122, USA  
<sup>48</sup>Texas A&M University, College Station, Texas 77843, USA  
<sup>49</sup>University of Texas, Austin, Texas 78712, USA  
<sup>50</sup>University of Houston, Houston, TX, 77204, USA  
<sup>51</sup>Tsinghua University, Beijing 100084, China  
<sup>52</sup>United States Naval Academy, Annapolis, MD 21402, USA  
<sup>53</sup>Valparaiso University, Valparaiso, Indiana 46383, USA  
<sup>54</sup>Variable Energy Cyclotron Centre, Kolkata 700064, India  
<sup>55</sup>Warsaw University of Technology, Warsaw, Poland  
<sup>56</sup>University of Washington, Seattle, Washington 98195, USA  
<sup>57</sup>Yale University, New Haven, Connecticut 06520, USA  
<sup>58</sup>University of Zagreb, Zagreb, HR-10002, Croatia

(Dated: December 3, 2024/ Revised version: V9d)

We report the first measurements of the moments — mean ( $M$ ), variance ( $\sigma^2$ ), skewness ( $S$ ) and kurtosis ( $\kappa$ ) — of the net-charge multiplicity distributions at mid-rapidity in Au+Au collisions at seven energies, ranging from  $\sqrt{s_{\text{NN}}} = 7.7$  to 200 GeV, as a part of the Beam Energy Scan program at RHIC. The moments are related to the thermodynamic susceptibilities of net-charge, which are

expected to diverge at the QCD critical point. We compare the products of the moments,  $\sigma^2/M$ ,  $S\sigma$  and  $\kappa\sigma^2$  with the expectations from Poisson and negative binomial distributions (NBD). The  $S\sigma$  values deviate from Poisson and are close to NBD baseline, while the  $\kappa\sigma^2$  values tend to lie between the two. Within the present uncertainties, our data do not show clear evidence of non-monotonic behavior as a function of collision energy.

PACS numbers: 25.75.-q, 25.75.Gz, 25.75.Nq, 12.38.Mh

The major goals of the physics program at Brookhaven National Laboratory's Relativistic Heavy-Ion Collider (RHIC) are the search and study of a new form of matter known as the Quark-Gluon Plasma (QGP) [1] and the mapping of the Quantum Chromodynamics (QCD) phase diagram in terms of temperature ( $T$ ) and baryon chemical potential ( $\mu_B$ ). Lattice QCD calculations indicate that at vanishing  $\mu_B$ , the transition from the QGP to a hadron gas is a smooth crossover, while at large  $\mu_B$ , the phase transition is of first order [2–8]. Therefore, a critical point in the QCD phase diagram is expected at finite  $\mu_B$ , where the first order transition ends. The location of the critical point has been predicted to be accessible at RHIC [9], where the beam energy scan program has been ongoing since 2010. The aim of this program is to map the QCD phase by varying the center-of-mass energy of the colliding ions, thereby scanning a large window in  $\mu_B$  and  $T$ .

One of the characteristic signatures of the QCD critical point is the non-monotonic behavior in the fluctuations of the charged particle multiplicity [4–14]. Fluctuations of the net-charge distributions have an advantage over other measured distributions, such as net-proton or net-kaon, because they directly probe a conserved quantum number [13–15]. Lattice and other QCD-based models suggest that the moments such as mean ( $M$ ), standard deviation ( $\sigma$ ), skewness ( $S$ ) and kurtosis ( $\kappa$ ), of the net-charge distributions are related to the corresponding higher-order thermodynamic susceptibilities and to the correlation length ( $\xi$ ) of the system [4–8, 14–17]. For example, the variance, skewness and kurtosis of the distributions are related to  $\xi^2$ ,  $\xi^{4.5}$  and  $\xi^7$ , respectively [16]. At the critical point, thermodynamic susceptibilities and the correlation length of the system diverge. When relating the susceptibilities to the moments, a volume term appears, making it difficult to compare different systems and collision centralities. The products of the moments, such as  $\sigma^2/M$ ,  $S\sigma$  and  $\kappa\sigma^2$ , are constructed in order to cancel the volume term. These products, as a function of beam energy and centrality, are expected to show non-monotonic behavior near the critical point [10, 18]. It has been recently proposed that experimental values of the products of the moments can be directly compared to lattice calculations in order to extract the freeze-out parameters of the produced system [19, 20]. Thus the moments of net-charge distributions provide a vital connection between experiment and lattice theory to probe the critical point.

In this letter, we report the first measurements of the moments of the net-charge multiplicity distributions in Au+Au collisions at  $\sqrt{s_{NN}} = 7.7, 11.5, 19.6, 27, 39, 62.4$  and 200 GeV, corresponding to  $\mu_B$  from 410 MeV to 20 MeV [21].

The data were taken by the Solenoid Tracker at RHIC (STAR) experiment in 2010 and 2011, as part of the Beam Energy Scan program at RHIC [9, 10, 22, 23]. With large uniform acceptance and excellent particle identification capabilities, STAR provides an ideal environment for studying event-by-event distributions of charged particles. The Time Projection Chamber (TPC) [24] is the main tracking detector used to identify charged particles and obtain net-charge (difference between the number of positive and negative charged particles) on an event-by-event basis. Combination of signals from the Zero Degree Calorimeters (ZDCs) [25], Vertex Position Detectors (VPDs) [26] and Beam-Beam Counters (BBCs) [27] are used as the minimum-bias trigger. The data analysis has been carried out for collisions occurring within  $\pm 30$  cm of the TPC center in the beam direction. Interactions of the beam with the beam pipe are rejected by selecting events with a radial vertex position in the transverse plane of less than 2 cm. The charged tracks are selected with more than 20 space points in the TPC out of 45, a distance of closest approach (DCA) to the primary vertex of less than 1 cm and number of hit points used to calculate the specific energy loss greater than 10. The spallation protons, produced due to beam-pipe interactions, affect the charged particle measurement. These are suppressed by removing protons with transverse momentum ( $p_T$ ) less than 400 MeV/ $c$ . To be consistent, anti-protons are also removed within this  $p_T$  range. The centrality of the collision is determined by using the total number of charged particles within a pseudorapidity ( $\eta$ ) window of  $0.5 < |\eta| < 1.0$ , chosen to be beyond the analysis window of the net-charge distributions. The centrality is represented by the average number of participating nucleons ( $\langle N_{\text{part}} \rangle$ ) as well as percentage of total cross section, obtained by the Monte Carlo (MC) Glauber simulation [28]. The total number of events analyzed are (in millions) 1.4, 2.4, 15.5, 24, 56, 32 and 75 for  $\sqrt{s_{NN}} = 7.7, 11.5, 19.6, 27, 39, 62.4$  and 200 GeV, respectively.

The measured number of positive ( $N_+$ ) and negative ( $N_-$ ) charged particles within  $|\eta| < 0.5$  and  $0.2 < p_T < 2.0$  GeV/ $c$  (after removing protons and anti-protons with  $p_T < 400$  MeV/ $c$ ) is used to calculate net-charge ( $N_+ - N_-$ ) in each event. The moments of the net-charge

distributions, obtained for a given centrality and beam energy may get affected by the volume variation because of finite centrality bin width. This effect is minimized by using the centrality-bin-width correction method outlined in Ref. [29]. The measured cumulants and moments are affected by the finite reconstruction efficiency. The efficiency for each centrality and collision energy is obtained by using the embedding technique. The average efficiencies vary within 63%–66% and 70%–73% for most central (0–5% bin) and peripheral (70–80% bin) events, respectively, for all collision energies. The corrections to the moments are based on binomial probability distributions of efficiency [13].

The statistical errors of the moments and their products have been calculated using the Delta theorem approach [30] and Bootstrap method [31] for efficiency-uncorrected and corrected results, respectively. The systematic uncertainties are obtained by varying the track selection criteria of the charged particles, such as the number of fit points, DCA, and the number of hit points used to calculate  $dE/dx$  in the TPC. For the efficiency-corrected results, final systematic errors were estimated by including an additional 5% uncertainty in the reconstruction efficiency.

In Fig. 1, the efficiency-corrected moments of the net-charge distributions are plotted as a function of  $\langle N_{\text{part}} \rangle$  for Au+Au collisions at seven c.m. energies. The statistical errors dominate in most cases and the systematic errors are within the symbol size. For all the collision energies, we observe that the  $M$  and  $\sigma$  values increase, whereas  $S$  and  $\kappa$  values decrease with increasing  $\langle N_{\text{part}} \rangle$ . The centrality dependence of the moments can be understood in terms of the central limit theorem (CLT), which assumes that each of the collisions is a collection of a finite number of identical, independent emission sources [32, 33]. Under this assumption,  $\langle N_{\text{part}} \rangle$  can be considered as a proxy for the volume of the system at a given centrality. The resulting CLT curves are superimposed in Fig. 1. The  $\chi^2/\text{ndf}$  values for the CLT fitting are found to be less than 2.0 in all cases, implying that the centrality dependence of the moments follows the general expectations from the CLT.

In order to understand the nature of moments and their products, it is essential to compare the results with baseline measures. Two such measures, one using the Poisson distribution and the other the negative binomial distribution (NBD), have been studied. In the case of the Poisson baseline, the positive and negative charged particle distributions are independently constructed from the measured mean values of these distributions. The resulting net-charge distributions are Skellam distributions [34]. For the NBD baseline, the positive and negative charged particle distributions are independently constructed by using both the measured means and variances. The expressions for the moments of the net-charge distributions for the NBD baseline may be found

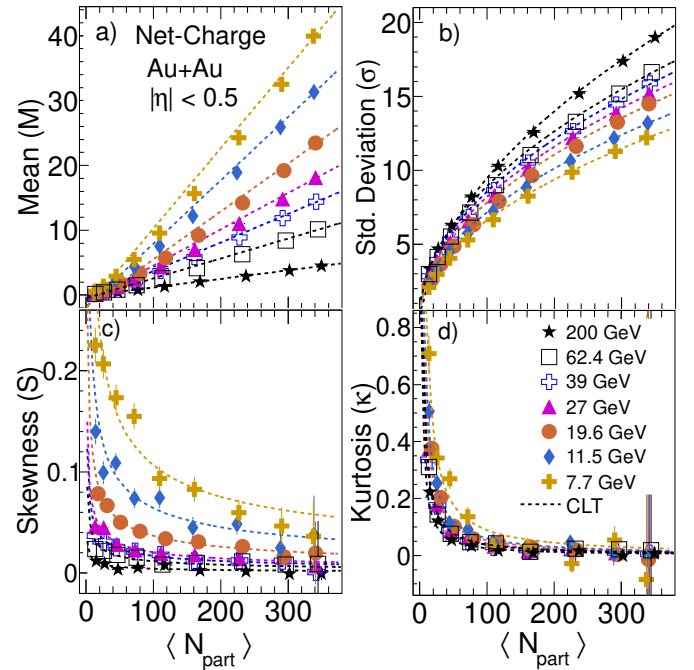


FIG. 1: (Color online) The efficiency-corrected (a) mean, (b) standard deviation, (c) skewness and (d) kurtosis of the net-charge multiplicity distributions as a function of number of participating nucleons ( $\langle N_{\text{part}} \rangle$ ) for Au+Au collisions at seven c.m. energies. The dotted lines represent the expectation from the central limit theorem. The error bars are the statistical errors and the systematic errors are within the symbol sizes.

in Ref. [35]. These baselines may provide adequate references for the moments of the net-charge distributions. Deviations from the baseline values may imply the presence of dynamical correlations and may help to observe possible non-monotonic behavior.

Figures 2 and 3 show the values of  $S\sigma$  and  $\kappa\sigma^2$ , respectively, plotted as functions of  $\langle N_{\text{part}} \rangle$  for Au+Au collisions at each of the seven collision energies. Both the efficiency-corrected and uncorrected results are shown for the experimental data points. The corrected results have larger statistical uncertainties than the uncorrected results because the efficiency corrections involve higher-order cumulants. Results from efficiency-corrected baselines are superimposed in both figures.

The  $S\sigma$  values, shown in Fig. 2, systematically decrease with increasing beam energy for all centralities. The differences between the Poisson and NBD baselines are small at  $\sqrt{s_{\text{NN}}} = 200$  GeV, and increase with decreasing beam energy. For low energies ( $\sqrt{s_{\text{NN}}} \leq 27$  GeV), the data are systematically above the Poisson baselines by more than two standard deviations. The NBD baselines give a better description of the data. Figure 3 shows that the values of  $\kappa\sigma^2$  at all energies and centralities are consistently larger than the Poisson baselines and below

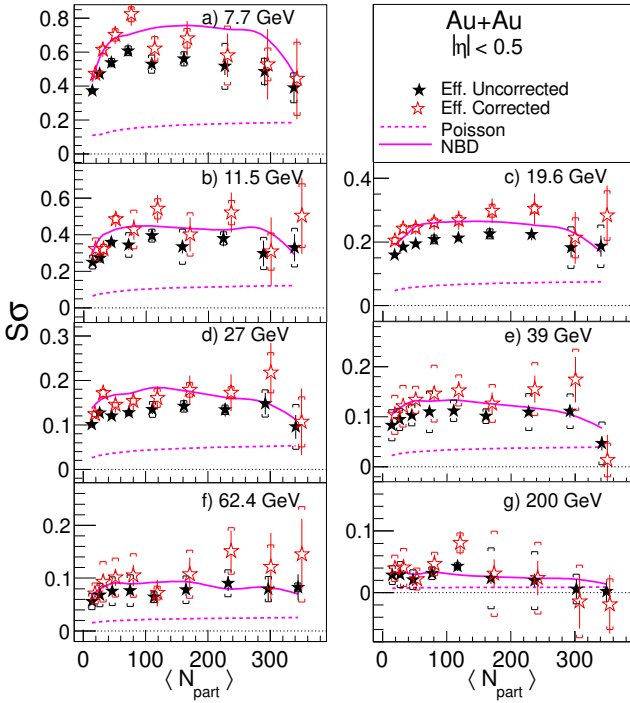


FIG. 2: (Color online) Both efficiency-corrected and uncorrected values of  $S\sigma$  as a function of  $\langle N_{\text{part}} \rangle$  for Au+Au collisions at  $\sqrt{s_{\text{NN}}} = 7.7$  to 200 GeV. The efficiency-corrected data points are shifted along the  $x$ -axis for better representation. Results from the Poisson and the NBD baselines are superimposed. The error bars are statistical errors and the caps represent systematic errors.

the NBD baselines.

In Fig. 4, we compare the beam-energy dependence of  $\sigma^2/M$ ,  $S\sigma$  and  $\kappa\sigma^2$  for two centrality bins, one corresponding to most central (0-5% bin) and the other to peripheral (70-80% bin) collisions. Results from the Poisson and NBD baselines are superimposed. All the results shown in this figure are corrected for reconstruction efficiencies. The values of  $\sigma^2/M$  are observed to increase with increasing beam energy, and are larger for peripheral collisions compared to the central collisions. In general, both baseline calculations overestimate the data. The  $S\sigma$  values are close to zero for  $\sqrt{s_{\text{NN}}} = 200$  GeV. These data points increase with decreasing beam energy for both centralities. The Poisson baselines underestimate the  $S\sigma$  values for most of cases, whereas the NBD baselines are close to the data. The  $\kappa\sigma^2$  values for the peripheral collisions show almost no variation as a function of beam energy, and lie above the Poisson baseline and below the NBD baseline. The values of  $\kappa\sigma^2$  for Poisson baseline is unity for all centralities. The statistical errors for the  $\kappa\sigma^2$  values in central collisions are presently large. Within these errors, the  $\kappa\sigma^2$  values at all energies are similar to each other. For central collisions at  $\sqrt{s_{\text{NN}}} = 7.7$  GeV, both baselines overestimate the data,

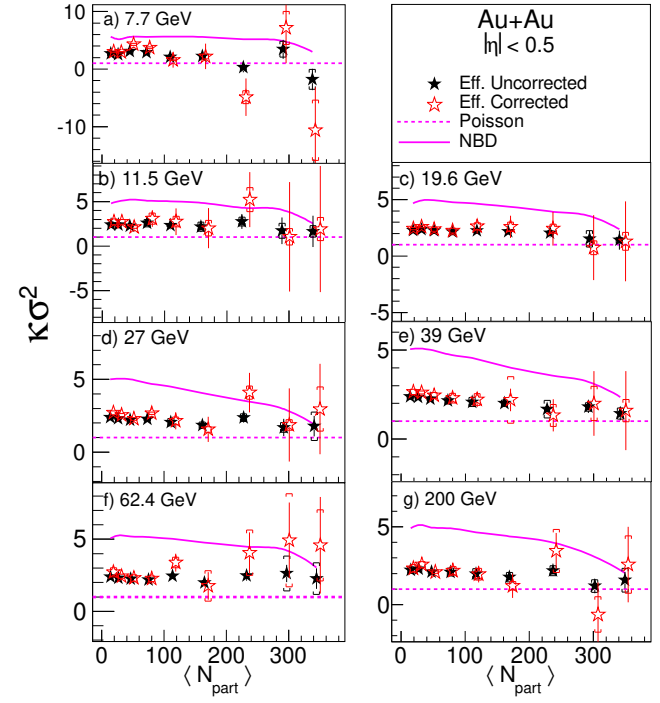


FIG. 3: (Color online) Both efficiency-corrected and uncorrected values of  $\kappa\sigma^2$  as a function of  $\langle N_{\text{part}} \rangle$  for Au+Au collisions at  $\sqrt{s_{\text{NN}}} = 7.7$  to 200 GeV. The efficiency-corrected data points are shifted along the  $x$ -axis for better representation. Results from the Poisson and the NBD baselines are superimposed. The error bars are statistical errors and caps represent systematic errors.

but are within two standard deviations.

Future measurements with higher statistics, especially at energies below 39 GeV, are needed to further constrain the results on  $S\sigma$  and  $\kappa\sigma^2$ . Present hardware upgrades of the STAR detector will facilitate such measurements. Final state effects, such as resonance decay and collision dynamics, may affect the interpretation of the measurements. Model comparisons, including those of the hadron resonance gas, will need to consider resonance decays with proper detector acceptance and kinematic cuts [32, 36–38].

In summary, the first results of the moments of net-charge multiplicity distributions for  $|\eta| < 0.5$  as a function of centrality for Au+Au collisions at seven collision energies from  $\sqrt{s_{\text{NN}}} = 7.7$  to 200 GeV are presented. These data can be used to explore the nature of the QCD phase transition and to locate the QCD critical point. We observe that the  $\sigma^2/M$  values increase monotonically with increasing beam energy. Weak centrality dependence is observed for both  $S\sigma$  and  $\kappa\sigma^2$  at all energies. The  $S\sigma$  values increase with decreasing beam energy. These values deviate from Poisson baseline, but are close to NBD baseline. The values of  $\kappa\sigma^2$  are observed to be within the two baseline distributions. Within the present

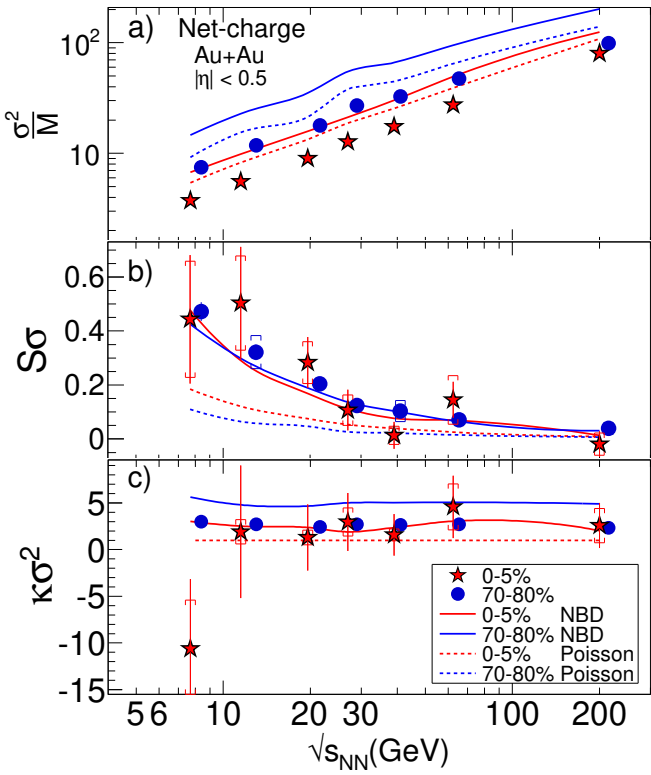


FIG. 4: (Color online) Beam-energy dependence of (a)  $\sigma^2/M$ , (b)  $S\sigma$ , and (c)  $\kappa\sigma^2$ , after all corrections, for most central (0-5%) and peripheral (70-80%) bins. The error bars are statistical errors and the caps represent systematic errors. Results from the Poisson and the NBD baselines are superimposed. The values of  $\kappa\sigma^2$  for Poisson baseline is unity for all centralities.

uncertainties, no non-monotonic behavior has been observed in the products of moments as a function of collision energy. Future realistic model calculations including proper kinematic cuts and final state effects are essential for comparison with measured data to investigate freeze-out parameters and the possible existence of a critical point.

We thank M. Asakawa, R. Gavai, S. Gupta, F. Karsch, V. Koch, S. Mukherjee, K. Rajagopal, K. Redlich and M. A. Stephanov for discussions related to this work. We thank the RHIC Operations Group and RCF at BNL, and the NERSC Center at LBNL, the KISTI Center in Korea and the Open Science Grid consortium for providing resources and support. This work was supported in part by the Offices of NP and HEP within the U.S. DOE Office of Science, the U.S. NSF, CNRS/IN2P3, FAPESP/CNPq of Brazil, Ministry of Ed. and Sci. of the Russian Federation, NNSFC, CAS, MoST, and MoE of China, the Korean Research Foundation, GA and MSMT of the Czech Republic, FIAS of Germany, DAE, DST, and CSIR of the Government of India, National Science

Centre of Poland, National Research Foundation (NRF-2012004024), Ministry of Sci., Ed. and Sports of the Rep. of Croatia, and RosAtom of Russia.

- 
- [1] J. Adams *et al.* (STAR Collaboration), Nucl. Phys. **A 757**, 102 (2005).
  - [2] Y. Aoki *et al.*, Nature **443**, 675 (2006).
  - [3] E. S. Bowman and J. I. Kapusta, Phys. Rev. **C 79**, 015202 (2009).
  - [4] S. Ejiri, Phys. Rev. **D 78**, 074507 (2008).
  - [5] Z. Fodor and S.D. Katz, JHEP04, 50 (2004).
  - [6] R. V. Gavai, S. Gupta, Phys. Rev. **D 78**, 114503 (2008).
  - [7] M. Cheng *et al.*, Phys. Rev. **D 77**, 014511 (2008).
  - [8] M. A. Stephanov, Prog. Theor. Phys. Suppl. **153**, 139 (2004); Int. J. Mod. Phys. **A 20**, 4387 (2005).
  - [9] M. M. Aggarwal *et al.* (STAR Collaboration), arXiv:1007.2613 [nucl-ex].
  - [10] M. M. Aggarwal *et al.* (STAR Collaboration), Phys. Rev. Lett. **105**, 022302 (2010).
  - [11] M. A. Stephanov, K. Rajagopal and E. V. Shuryak, Phys. Rev. Lett. **81**, 4816 (1998).
  - [12] P. Braun-Munzinger *et al.*, Nucl. Phys. **A 880**, 48 (2012).
  - [13] A. Bzdak and V. Koch, Phys. Rev. **C 86**, 044904 (2012).
  - [14] V. Skokov, B. Friman and K. Redlich, Phys. Lett. **B 708**, 179 (2012).
  - [15] M. Kitazawa and M. Asakawa, Phys. Rev. **C 85**, 021901 (2012).
  - [16] M.A. Stephanov, Phys. Rev. Lett. **102**, 032301 (2009).
  - [17] M. Asakawa, S. Ejiri, and M. Kitazawa, Phys. Rev. Lett. **103**, 262301 (2009).
  - [18] L. Adamczyk *et al.* (STAR Collaboration), Phys. Rev. Lett. **112** 032302 (2014).
  - [19] A. Bazavov *et al.*, Phys. Rev. Lett. **109**, 192302 (2012).
  - [20] S. Borsanyi *et al.*, Phys. Rev. Lett. **111**, 062005 (2013).
  - [21] J. Cleymans *et al.*, Phys. Rev. **C 73**, 034905 (2006).
  - [22] D. McDonald, Ph.D. thesis, Rice University, 2013.
  - [23] N.R. Sahoo, Ph.D. thesis, Homi Bhabha National Institute, 2013.
  - [24] M. Anderson *et al.*, Nucl. Instrum. Meth. **A 499**, 659 (2003).
  - [25] C. Adler *et al.*, Nucl. Instrum. Methods **A 470**, 488 (2001).
  - [26] W. J. Llope *et al.*, Nucl. Instrum. Methods **A 522**, 252 (2004).
  - [27] C. A. Whitten, AIP Conf. Proc. **980**, 390 (2008).
  - [28] M. L. Miller *et al.*, Ann. Rev. Nucl. Part. Sci. **57**, 205 (2007).
  - [29] X. Luo, J. Xu, B. Mohanty and N. Xu, Nucl. Part. Phys. **40**, 105104 (2013).
  - [30] X. Luo, J. Phys. G: Nucl. Part. Phys. **39**, 025008 (2012).
  - [31] B. Efron, Computers and the Theory of Statistics: Thinking the Unthinkable; SIAM Review, Published by Society for Industrial and Applied Mathematics (url: <http://www.jstor.org/stable/2030104>.)
  - [32] N. R. Sahoo, S. De and T. K. Nayak, Phys. Rev. **C 87**, 044906 (2013).
  - [33] X. F. Luo, B. Mohanty, H. G. Ritter and N. Xu, J. Phys. **G 37**, 094061 (2010).
  - [34] The difference of two independent Poisson distributions is a Skellam distribution, for which  $\frac{\sigma^2}{M} = \frac{\langle N_+ \rangle + \langle N_- \rangle}{\langle N_+ \rangle - \langle N_- \rangle}$ ,

- $S\sigma = \frac{\langle N_+ \rangle - \langle N_- \rangle}{\langle N_+ \rangle + \langle N_- \rangle}$ , and  $\kappa\sigma^2 = 1$ .
- [35] T.J. Tarnowsky and G.D. Westfall, Phys. Lett. **B** **724**, 51 (2013).
- [36] S. Jeon and V. Koch, Phys. Rev. Lett. **85**, 2076 (2000).
- [37] F. Karsch and K. Redlich, Phys. Lett. **B** **695**, 136 (2011).
- [38] P. Garg, D. K. Mishra, P. K. Netrakanti, B. Mohanty, A. K. Mohanty, B. K. Singh and N. Xu, Phys. Lett. **B** **726**, 691 (2013).